The variability of Amazonian palm phytoliths

Witteveen, N.H.; Hobus, C.E.M.; Philip, A.; Piperno, D.R.; McMichael, C.N.H.

DOI
10.1016/j.revpalbo.2022.104613
Publication date
2022
Document Version
Final published version
Published in
Review of Palaeobotany and Palynology

Review of Palaeobotany and Palynology 300 (2022) 104613

Contents lists available at ScienceDirect

Review of Palaeobotany and Palynology

journal homepage: www.elsevier.com/locate/revpalbo

The variability of Amazonian palm phytoliths

N.H. Witteveen [a,*], C.E.M. Hobus [a], A. Philip [a], D.R. Piperno [b,c], C.N.H. McMichael [a]

[a] Department of Ecosystem and Landscape Dynamics, Institute for Biodiversity and Ecosystem Dynamics, University of Amsterdam, Science Park 904, 1098 GE Amsterdam, Netherlands
[b] Department of Anthropology, Smithsonian National Museum of Natural History, Washington, DC 20560, United States of America
[c] Smithsonian Tropical Research Institute, Balboa, Ancon, Panama

ARTICLE INFO

Article history:
Received 16 September 2021
Received in revised form 21 January 2022
Accepted 23 January 2022
Available online 8 February 2022

Keywords:
Phytoliths
Palms
Arecaceae
Amazonia
Morphology
Palaeoecology

ABSTRACT

The Arecaceae (palm) family is one of the most common and economically important plant groups in Amazonia, and play large roles in ecosystem functioning and carbon dynamics. The modern dominance of palms may be a result of environmental gradients, past climate variability and legacies of past human activities. To understand the roles people and environment have played in shaping the abundance and widespread occurrence of Amazonian palm species, past vegetation reconstructions using palaeoecological proxies that can identify palm species or genera are needed. Phytoliths are siliceous microfossils abundantly produced in palms and are used to reconstruct past vegetation composition. The aim of this paper was to assess the variability of Amazonian palm phytolith morphotypes and to determine which morphological characteristics can be used to increase the taxonomic resolution of palm identifications. Phytolith size, sphericity, spinule traits and number of (surficial) projections were measured for 24 Amazonian palm species. Differences were compared using PCA and ANOVA or Tukey tests, followed by Kruskal-Wallis or Dunn tests. Results show potential for phytoliths of *Aiphanes aculeata, Attalea maripa, Bactris simplicifrons, Dictyocaryum fuscum, Euterpe precatoria, Iriartea deltoidea, Oenocarpus bacaba, Socratea exorrhiza* and the genera **Geonoma, Bactris, Euterpe** and **Oenocarpus** to be identified based on their size, shape or number of projections. This will allow future phytolith analyses to reconstruct past palm abundances with an increased taxonomic resolution. We have formulated our findings into a 'quick guide' to identify palm phytoliths and test hypotheses regarding the drivers of modern palm distributions and abundances.

1. Introduction

Palms are a common component of the Amazon rainforest: 20 palm species are among the 227 'hyperdominant' tree species that account for more than half of the individuals in the forest(Ter Steege et al., 2013; ter Steege et al., 2020). Their high abundances mean that palms play a large role in Amazonia's carbon dynamics (Fauset et al., 2015; Muscarella et al., 2020). Abiotic factors such as climate, soil, topography, hydrology, dispersal and physiological adaptations have shaped palm distributions in Amazonia (Eiserhardt et al., 2011; Kristiansen et al., 2009; Vormisto et al., 2004). Also, animal abundances, particularly of seed dispersers, affect palm abundances and distributions (Eiserhardt et al., 2011) (Goulding et al., 2007). It is hypothesized that modern palm abundances across Amazonia are a legacy of past human activities, particularly during the pre-Columbian era (Levis et al., 2017), because palms were well-exploited (e.g., Morcote-Rios and Bernal, 2001). For example, *Bactris gasipaes*, the peach or *pehibaye* palm, was domesticated (Clement, 1988). Still today, people in Amazonia use at least 134 of 225 different palm species for food, construction, tools and cultural practices (Macia et al., 2011). Existing data from the prehistoric period reveal variability in the extent to which ancient people may have influenced modern palm abundance in Amazonia. In some regions, palms that grew near human settlements increased in abundance (Maezumi et al., 2018; McMichael et al., 2015), while decreasing in others (Åkesson et al., 2021). Palm abundance has also increased or remained largely unchanged in areas where human impacts were minimal (Heijink et al., 2020; McMichael et al., 2021; Piperno et al., 2021).

To understand the roles people and environment have played in shaping the abundance and widespread occurrence of Amazonian palm species, past vegetation reconstructions using palaeoecological proxies that can identify palm species or genera are needed. Phytoliths (silica microfossils) are used to reconstruct past vegetation composition and are produced abundantly in most palm species (Piperno, 2006). Phytoliths are usually not dispersed by wind, but instead provide a local signal of the vegetation (±30 m) in both soils and lake sediments (Piperno, 1989; Åkesson et al., 2021). Phytolith analysis can be carried out in areas where pollen degrades, such as terrestrial soils (McMichael et al., 2012), or used to complement pollen reconstructions in lake sediments (Åkesson et al., 2021; Maezumi et al., 2018).

* Corresponding author at: University of Amsterdam, 904 Science Park, 1098 GE Amsterdam, Netherlands.
E-mail address: n.h.witteveen@uva.nl (N.H. Witteveen).

https://doi.org/10.1016/j.revpalbo.2022.104613

Palms (ARACACEAE) usually make either spheroid or conical phytoliths with an echinate texture (Tomlinson, 1961; Piperno, 1989, 2006). ARACACEAE phytoliths from South America can be visually separated from other monocotyledon families (BROMELIACEAE, CANNACEAE, MARANTACEAE, ORCHIDACEAE, STRELITZIACEAE, and ZINGIBERACEAE) based on differences in the morphotypes produced and the morphological variation of spheroid echinates (Benvenuto et al., 2015; Chen and Smith, 2013; Piperno, 2006, 1989). But the strong overlap of morphological variables (such as size) between palm species makes it difficult to increase taxonomic resolution to the species level (Neumann et al., 2019).

An assemblage-based approach may allow to distinguish some palm taxa, either based on morphometrical analysis (Fenwick et al., 2011) or on the relative frequency of morphotypes (Benvenuto et al., 2015). Within the ARACACEAE family, subfamilies Coryphoideae and Arecoideae can be distinguished based on morphological differences of spheroid echinate phytoliths (Benvenuto et al., 2015). On a genus level, **Geonoma** produces diagnostic conical phytoliths (Morcote-Ríos et al., 2016) and **Euterpe** and **Oenocarpus** produce large spheroid phytoliths with acute projections (SPH_ACU) with a larger size than other species (Morcote-Ríos et al., 2016; Piperno and McMichael, 2020). Recent studies showed phytoliths produced by South American palm species can be differentiated into 5 taxonomically relevant spheroid echinate morphotypes, 4 conical echinate morphotypes and reniform phytoliths (Huisman et al., 2018; Morcote-Ríos et al., 2016). Morphometrical analyses of palm phytoliths in other regions also showed differences between species in size, shape, or spinule traits (Delhon and Orliac, 2010; Fenwick et al., 2011).

However, a detailed morphometric analysis on spheroid echinate and conical palm phytoliths from South America is missing, because studies either measured a limited number of species (Benvenuto et al., 2015; Delhon and Orliac, 2010) or used a descriptive approach for a large reference collection (Huisman et al., 2018; Morcote-Ríos et al., 2016; Watling and Iriarte, 2013). Perhaps because there is no general agreement on what diagnostic features lower taxonomic resolution, most studies count only 1 conical morphotype and few spheroid morphotypes of palms in fossil records (Åkesson et al., 2021; Piperno et al., 2021; Whitney et al., 2014). Increasing the taxonomic resolution of palm phytoliths will improve vegetation reconstructions, making it possible to study the drivers of modern palm distributions in Amazonia.

The aim of this paper is to answer the following research questions:

(1) What is the variability of phytolith morphology in 24 Amazonian palm species?

(2) Which morphological characteristics of phytoliths can be used to increase taxonomic identification of palms in palaeoecological reconstructions?

To standardize and improve the taxonomic resolution of phytolith studies in Amazonia, we investigate here whether a detailed morphometric analysis of phytoliths and the relative abundance of morphotype for each species may further differentiate palm taxa.

2. Material and methods

Reference material of 24 palm species was collected from the Leiden Herbarium and Hortus Botanicus Amsterdam (the Netherlands). Species focused on were hyperdominant (11 species) or useful for people (19 species), and 3 species had not been previously analyzed (Table 1). Specimens were sampled for leaves, woody parts, fruits, or seeds, depending on availability. All samples were processed according to standard laboratory procedures for wet processing (Piperno, 2006). Organic matter and carbonates were removed from the phytolith samples using 33% H_2O_2, $KMnO_4^-$ and 10% HCl. Phytoliths were extracted by heavy liquid flotation using Bromoform at a specific gravity of 2.3 (McMichael et al., 2021). Phytoliths were mounted on microscope slides using Naphrax and identified using immersion oil at 1000× magnification under a Zeiss Axioscope microscope

The relative abundance of morphotypes for each sample was calculated by counting a total of 300 palm phytoliths per slide (Table S1). Phytoliths were counted using morphological descriptions from the literature (e.g., Morcote-Ríos et al., 2016; Huisman et al., 2018), using the latest nomenclature (Table S2). For each sample, at least 30 phytoliths and for each morphotype at least 3 replicates per species were photographed and morphological characteristics were measured using Image J software (Abràmoff et al., 2004). The following numerical variables were measured for conical phytoliths: length (μm), width (μm), number of projections, length of spines (μm), width of spines (μm), distance between spines (μm) and sphericity (length/width). For spheroid phytoliths, the numerical variables measured were maximum diameter (μm), number of surficial projections, length of spines (μm), width of

Table 1
Experimental design showing species name, which part of the plant was used (leaf, seed, flower, fruit, woody or other), what phytolith morphotype was present and if the species is useful and/or hyperdominant.

Subfamily	Species	Plant part sampled	Phytoliths present	Useful (U), Hyperdominant (H)	Botanical specimen number
Arecoideae	*Aiphanes aculeata Wiild.*	Seed[a], woody	Conical	U	
Arecoideae	*Bactris gasipaes*	Flower[a]	Conical	U,H	
Arecoideae	*Bactris simplicifrons*	Leaf	Conical		
Ceroxyloideae	*Chamaedorea pinnatifrons*	Leaf	Conical		
Arecoideae	*Dictyocaryum fuscum*	Leaf, seed	Conical	U	
Arecoideae	*Dictyocaryum lamarckianum*	Long seed[a], Round seed[a]	No phytoliths, Malformed phytoliths	U	
Arecoideae	*Iriartea deltoidea*	Leaf	Conical	U,H	
Arecoideae	*Socratea exorrhiza*	Leaf	Conical	U,H	
Arecoideae	*Wettinia hirsuta*	Flower, seed	Conical		
Arecoideae	*Elaeis oleifera*	Leaf	Spheroid	U,H	
Arecoideae	*Geonoma undata*	Leaf, woody	Conical	U	
Arecoideae	*Geonoma paradoxa*	Leaf	Conical		
Arecoideae	*Geonoma maxima*	Leaf	Conical	U	
Arecoideae	*Attalea undiff.*	Unknown	Spheroid		
Arecoideae	*Attalea maripa*[a]	Leaf	Spheroid	U,H	U.0273828
Arecoideae	*Attalea speciosa*[a]	Leaf[a], woody[a]	Spheroid	U	U.1122243, U.1122246
Arecoideae	*Euterpe precatoria*	Leaf, seed, woody	Spheroid	U,H	
Arecoideae	*Euterpe catinga Wallace*	Leaf	Spheroid	U	
Arecoideae	*Hyospathe elegans*	Leaf	Spheroid	U	
Calamoideae	*Mauritia flexuosa*[a]	Leaf	Spheroid	U,H	U.1140014
Calamoideae	*Mauritiella armata*[a]	Leaf	Spheroid	U,H	U.1140064
Arecoideae	*Oenocarpus bataua*[a]	Leaf	Spheroid	U,H	WAG.1143694
Arecoideae	*Oenocarpus bacaba*[a]	Leaf	Spheroid	U,H	U.1124948
Arecoideae	*Oenocarpus mapora*	Leaf, other	Spheroid	U	

[a] Species or plant part that was not previously studied.

spines (μm), distance between spines (μm), sphericity (maximum diameter/perpendicular diameter) and perpendicular diameter (μm) according to Benvenuto et al. (2015).

2.1. Data analysis

Principal Components Analysis (PCA) was used to simultaneously assess the variability of all morphological measurements across species, to see if species would separate based on morphology and which variables contributed mostly to this separation. PCA were run separately within general morphotypes (e.g. within conical phytoliths and within spheroid phytoliths). Pearson correlation tests were used to see if measured characteristics were correlated within each morphotype separately. Because several variables were correlated, and most variables were not normally distributed, we conducted pairwise comparisons between species, for each variable separately. For all variables, mean differences between the measured morphological characteristics of species were tested using ANOVA and Tukey tests, or Kruskal-Wallis and Dunn tests (when residuals were not normally distributed). We adjusted p-values with the Benjamini-Hochberg method because multiple comparisons were made on the same dataset. The pairwise comparisons were used to assess for each variable separately the amount of variation between and within a species, and the ranges of minimum and maximum values. The minimum sample size needed to accurately reflect mean values of each morphotype and species was calculated (Ball et al., 2016). Analyses were performed in R Studio Version 1.4.1103, colors were chosen using the 'viridis' package (Garnier et al., 2021) and the PCA was performed using the 'princomp' function of the 'stats' and 'factoextra' packages (Kassambara and Mundt, 2017). The full reproducible code is available in the Supplementary Material.

3. Results

3.1. Spheroid phytoliths

3.1.1. New morphotypes

Spheroid echinate phytoliths with very small or "undeveloped" spines were found in *Oenocarus mapora* (7–25%), *Oenocarpus bacaba* (17%), *Attalea speciosa* (12–36%) and *Attalea maripa* (30%) (Fig. 1-af, ai). These phytoliths had both spheroidal and ellipsoidal shapes like Spheroid echinate (SPH_ECH) and Ellipsoidal echinate (ELL_ECH) phytoliths, but with less pronounced projections and a texture that appeared more tuberculate. These species also produced spheroid psilate and lobate psilate phytoliths (Collura and Neumann, 2017) (Fig. S4-z, aa, Table S1). Because all species produced both spheroidal and ellipsoidal shapes, all morphotypes with a "tuberculate" texture were grouped as "spheroid tuberculate (SPH_TUB)" for statistical comparisons.

Spheroid phytoliths with rounded projections (SPH_ROU) were found in *Oenocarpus bacaba* (5%) with a size range of 21–27 μm (Fig. S4-ae). The texture with rounded projections clearly distinguishes this morphotype from other spheroid phytoliths.

3.1.2. Relative abundance of spheroid phytoliths

Spheroid phytoliths were produced by **Euterpe, Oenocarpus, Attalea,** *Eleais oleifera, Hyospathe elegans, Mauritia flexuosa* and *Mauritiella armata* (Figs. 1, 2). Species differed in the frequency and type of morphotypes they produced: *Hyospathe elegans* and *Elaeis oleifera* produced mostly Ellipsoidal echinate (ELL_ECH) phytoliths, whereas *Mauritiella armata* produced mostly Spheroid echinate (SPH_ECH) phytoliths. More than 70% of phytoliths produced by *Euterpe* and *M. flexuosa* were Spheroid echinate symmetrical (SPH_SYM) phytoliths, *Euterpe precatoria, Oenocarpus bataua* and *Oenocarpus bacaba* produced SPH_SYM phytoliths between 12 and 46% and other species produced SPH_SYM phytoliths rarely (<3%). SPH_TUB and spheroid psilate phytoliths were produced only by **Oenocarpus** and **Attalea** species, and very rarely occurred in *Euterpe precatoria* and *M. flexuosa* (<1%). Reniform phytoliths were produced by *Attalea, Oenocarpus, Euterpe precatoria, Hyospathe elegans* and *E. oleifera* in small amounts of 1–5%. Spheroid acute projections (SPH_ACU) were produced by **Oenocarpus** and **Euterpe** in small amounts (3%).

3.1.3. Multivariate analysis of spheroid phytoliths

The first axis of the PCA (PCA1; eigenvalue = 3.9; 56% of the total variance) separated the larger phytoliths from the smaller ones (Fig. 3). For example, larger SPH_ACU phytoliths from **Euterpe** and **Oenocarpus** are on the positive PCA1 axis, along with the large SPH_SYM of *Oenocarpus bacaba*. Species that consistently produced smaller phytoliths, such as *Attalea speciosa, Elaeis oleifera* and *Mauritiella armata*, are on the negative PCA1 axis. *Attalea maripa* produced large phytoliths and is displayed on the positive PCA2 axis. The second axis (PCA2; eigenvalue = 1.3; 19% of the total variance) separated the phytoliths based on the number of surficial projections. Therefore, morphotypes SPH_SYM and SPH_TUB occupied space on the negative side of PCA2, whereas SPH_ACU phytoliths are on the positive PCA2 axis. The previously established morphotypes, shown as different colors in Fig. 3, are separated by the PCA, except for the overlap between SPH_TUB and other morphotypes.

3.1.4. Pairwise comparisons between species producing spheroid phytoliths

Most species producing spheroid phytoliths overlap in size, shape, spinule traits and number of surficial projections (Fig. S1, S2). Species differences between spinule traits resembled patterns of maximum and perpendicular diameter for all spheroid morphotypes except SPH_TUB phytoliths (Supplementary Material "Correlation"). Morphotype SPH_ACU was rare, therefore, for robust statistical analysis the sampling size of these morphotypes should be increased to 203 phytoliths (Supplementary Material "Robustness"). Also, the species that produced a mixture of small SPH_ECH and large SPH_ACU required large sampling sizes of at least 140 phytolith.

On average, the maximum diameter of ELL_ECH phytoliths (7-18 μm) of *Attalea maripa* was larger than other species. The average maximum diameter of SPH_ECH phytoliths (11–18 μm) of *Attalea maripa* was also larger than other species, but overlapped with the range of *Euterpe catinga, Mauritia flexuosa* and *Oenocarus bacaba* (Fig. S1). The average surficial projections of SPH_ECH phytoliths of *Mauritiella armata* (14) exceeded that of other species. For SPH_SYM phytoliths, *Oenocarpus bacaba* produced larger phytoliths ranging from 8 to 22 μm, which was significantly higher than other species, which were typically smaller than 15 μm, except *M. flexuosa.* The maximum diameter of SPH_ACU of **Euterpe** (7–37 μm) and **Oenocarpus** species (14–24 μm) was larger than other species, who typically did not exceed 20 μm. SPH_TUB morphotypes were produced by *Attalea maripa* with a maximum diameter that typically ranged from 9 to 17 μm, whereas the other species were typically smaller than 13 μm, except for *Oenocarpus bacaba*, who ranged from 7 to 15 μm (Fig. S1).

3.2. Conical phytoliths

3.2.1. Relative abundance of conical phytoliths

Conical phytoliths were produced by *Iriartea deltoidea, Socratea exorrhiza, Dictyocaryum fuscum, Chamaedorea pinnatifrons, Wettinia hirsuta, Aiphanes aculeatum,* **Bactris** and **Geonoma** species (Fig. 4 and Table S1). Species differed in the frequency and type of morphotypes they produced: all conical morphotypes produced by *Iriartea deltoidea, Socratea exorrhiza* and the leaves of *Dictyocaryum fuscum* were Conical few projections (CON_FEW) phytoliths (Fig. 4, Table S1). More than 89% of the phytoliths produced by **Bactris** species were CON_FEW phytoliths, and Conical echinate (CON_ECH) phytoliths were produced in low amounts of <8%. *Bactris simplicifrons* also produced Conical tabular (CON_TAB) phytoliths in low amounts of 3%. More than 40% of the phytoliths produced by *Wettinia hirsuta*, *Dictyocaryum fuscum* and

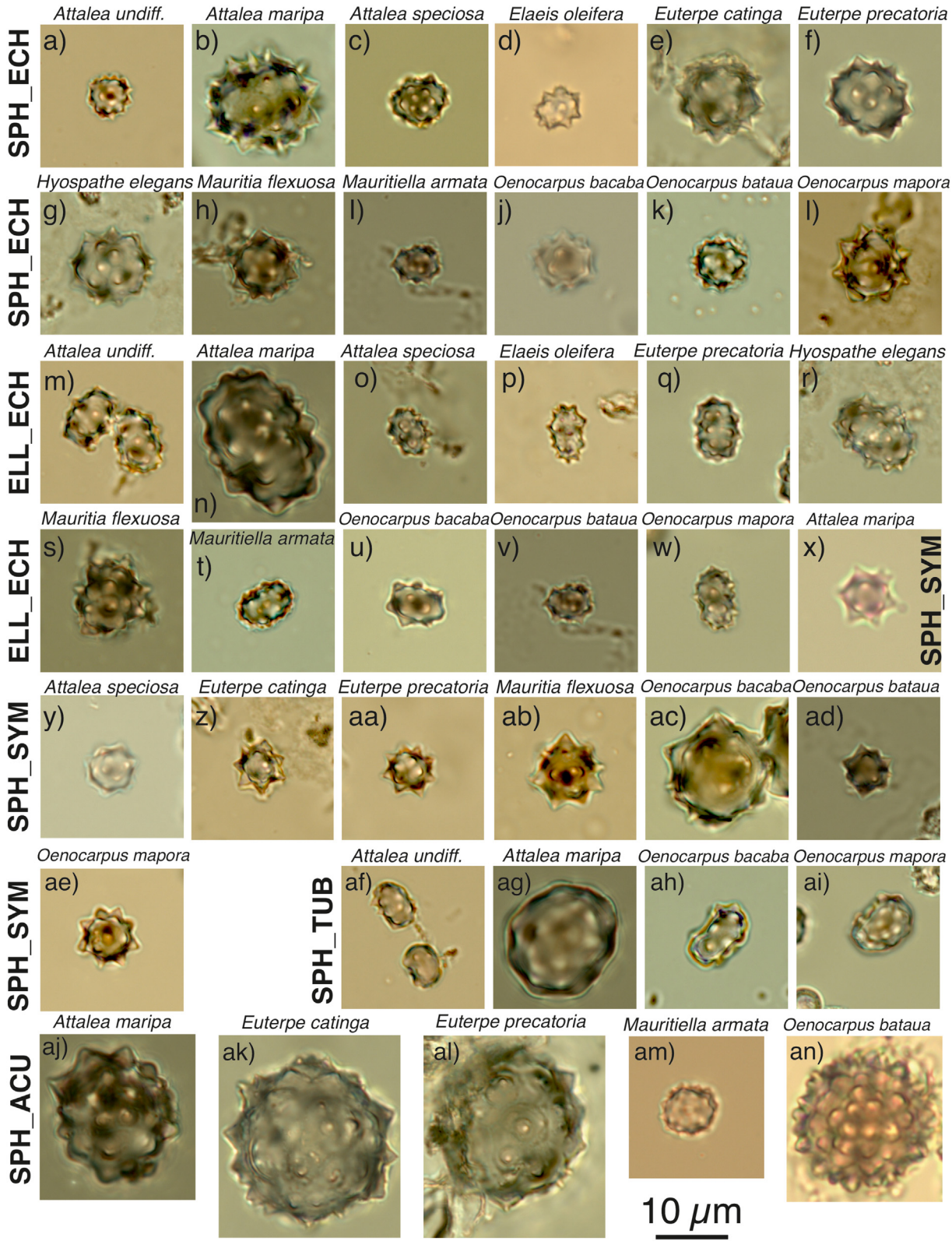

Fig. 1. Variability of spheroidal phytoliths produced by each species, with SPH_ECH phytoliths shown in panels a-l, ELL_ECH phytoliths in panels m-w, SPHEROID ECHINATE SYMMETRICAL (SPH_SYM) phytoliths in x-ae, SPH_TUB phytoliths in af-ai and SPHEROID ACUTE PROJECTIONS (SPH_ACU) phytoliths in panels aj-an.

Aiphanes aculeatea were CON_TAB phytoliths. CONICAL BASAL PROJECTIONS (CON_BAS) were produced by **Geonoma** species only. The woody samples of *Geonoma undata* also contained CON_TAB, FUSIFORM ECHINATE (FUS_ECH) and other phytoliths.

3.2.2. Multivariate analysis of conical phytoliths

The first axis of the PCA (PCA1; eigenvalue = 3.3; 47% of the total variance; Fig. 5) separated the phytoliths with a larger width, length and spine width from the smaller ones. For example, larger CON_FEW phytoliths

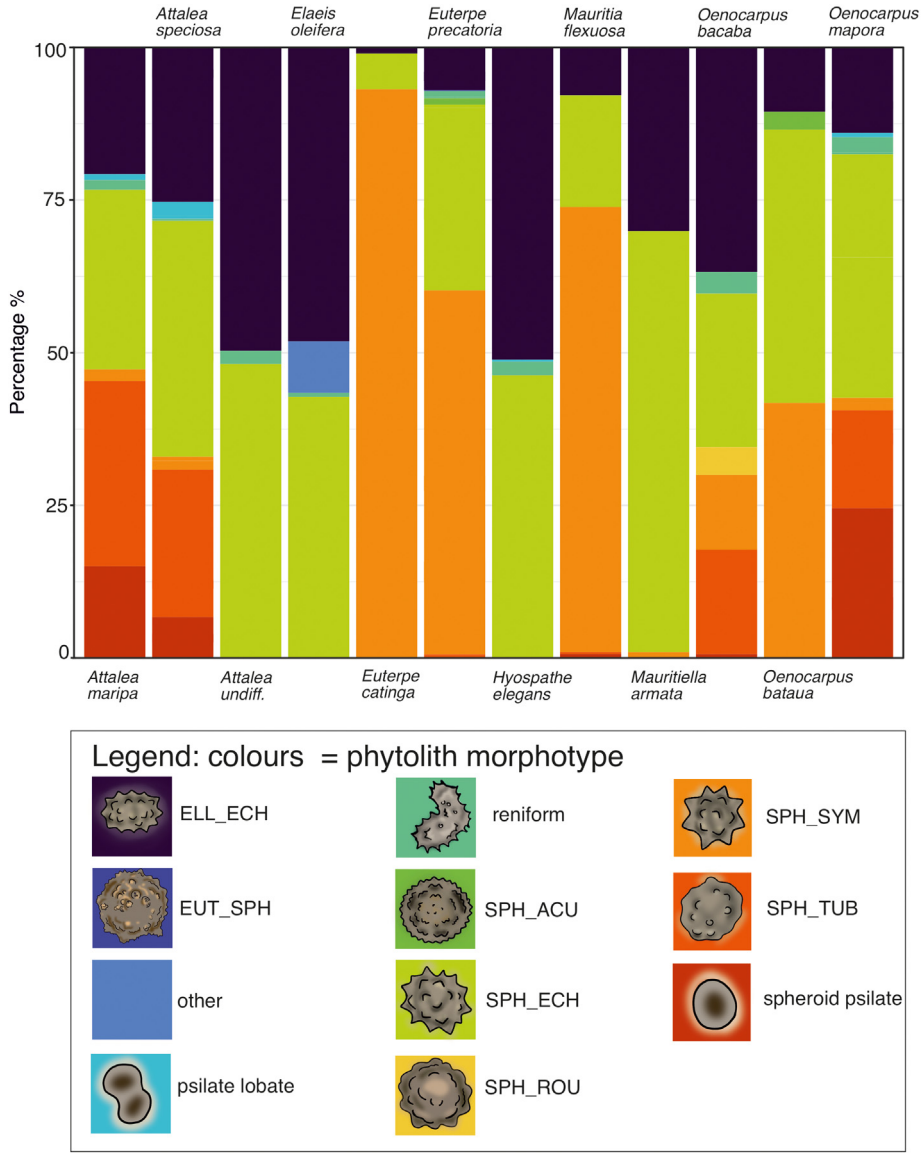

Fig. 2. Relative frequency of spheroid morphotypes is shown in percentage (%) on the y-axis, with colors showing different morphotypes, and each bar on the x-axis represents a specimen. Based on 300 counted phytoliths per sample.

from *Iriartea deltoidea* and *Socratea* exorrhiza are on the negative PCA1 axis, as well as large CON_ECH from **Bactris**. Species that consistently produced smaller phytoliths, such as *Geonoma undata* and *Aiphanes aculeatea*, are on the positive PCA1 axis. The second axis (PCA2; eigenvalue = 1.2; 17% of the total variance) separated the phytoliths based on sphericity and spine length. Therefore, CON_BAS is mostly on the negative side of PCA2 as well as the oblong CON_FEW of *Iriartea deltoidea,* and circular CON_FEW and CON_ECH phytoliths are occupying the positive PCA2. There is some overlap between CON_FEW and CON_ECH morphotypes and between CON_ECH and CON_TAB morphotypes. But overall, previously established morphotypes are separated by the PCA.

3.2.3. Pairwise comparisons between species producing conical phytoliths

Most species that produce conical phytoliths overlap in size, shape, and spinule traits (Supplementary material "Correlation"). But species differences between size were found for all conical morphotypes. Differences between shape and spinule traits stood out for CON_FEW, and differences in projections for CON_ECH. Morphotype FUS_ECH was rare, therefore, for robust statistical analysis the sampling size of this morphotype should be increased to 45 phytoliths (Supplementary material "Robustness"). Also, several species produced phytoliths with a wide range of length and width, resulting in a larger required sampling size for statistcal comparisons.

On average, CON_FEW phytoliths that were circular and larger than 12 μm were produced by *Socratea exorrhiza* and *Wettinia hirsuta*, and CON_FEW phytoliths that were oblong and larger than 12 μm were produced by *Iriartea deltoidea* (Fig. 6-de). A similar pattern was found for spine length and width: the size of *Iriartea deltoidea*, *Socratea exorrhiza* and *Wettinia hirsuta* typically exceeded 1 μm, whereas the spine length and width of other species was typically 1 μm or smaller (Fig. S3). *Dictyocaryum fuscum* produced smaller CON_FEW phytoliths, ranging from 8 to 10 μm, whereas other species were typically larger than 10 μm.

Bactris species produced CON_ECH phytoliths with significantly fewer projections (<9) compared to other species, who typically had >12 projections. Very large conical echinate phytoliths >17 μm with relatively few projections (7–9) were seen only in *Bactris simplicifrons* (Fig. 6-mn). On average, the length of CON_ECH phytoliths (6–11 μm) and CON_TAB phytoliths (7–12 μm) of *Aiphanes aculeata* were smaller than other species, except for *Chamaedorea pinnatifrons*, whose CON_ECH phytoliths ranged from 9 to 12 μm.

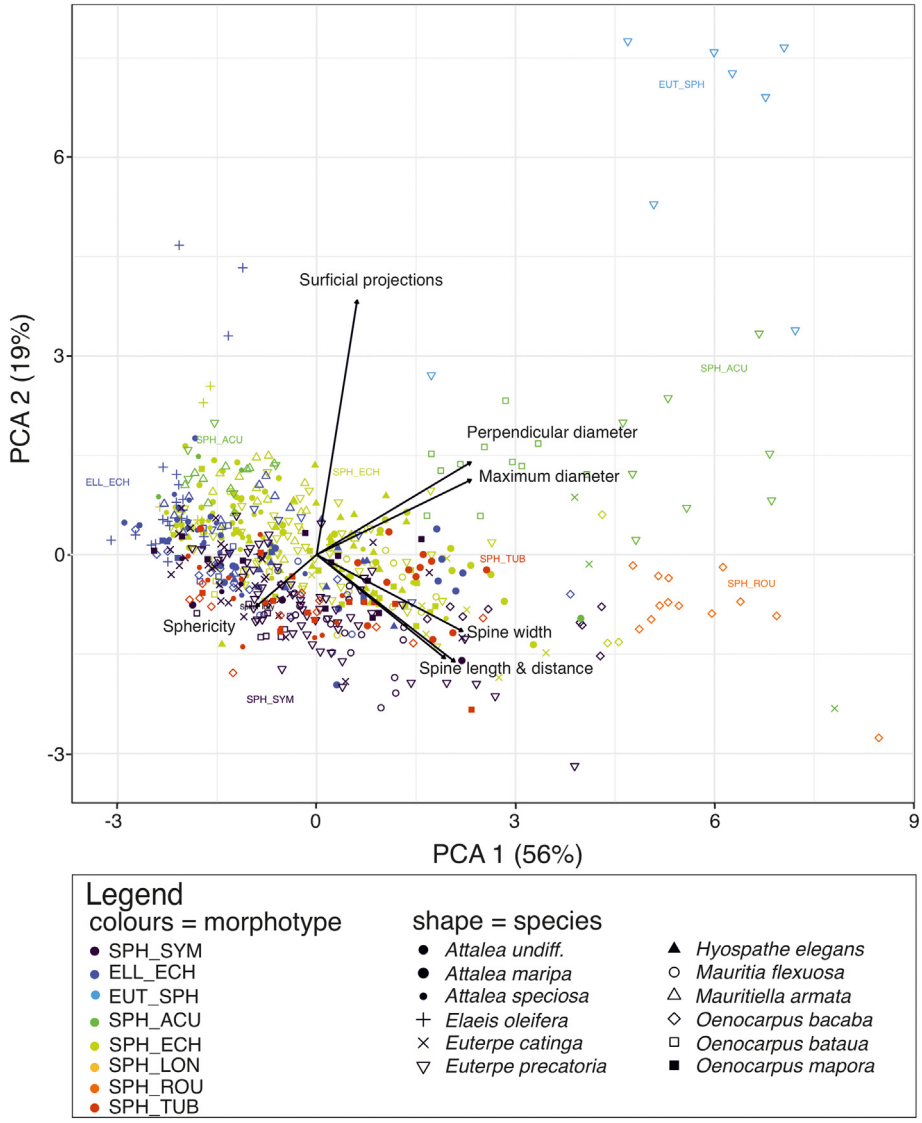

Fig. 3. PCA of spheroid phytoliths. PCA1 on the x-axis explains 56% of the variance found and PCA2 on the y-axis explains 19%. Different colors indicate spheroid morphotypes and different shapes indicate species.

Dictyocaryum fuscum produced CON_TAB phytoliths with a mean sphericity of 1.7, which was larger than *Geonoma undata* (1.2), but there were no significant differences between other species. The maximum diameter of CON_BAS phytoliths of *Geonoma undata* (5–13 μm), *Geonoma maxima* (9–14 μm) and *Geonoma paradoxa* (7–16 μm) all differed significantly from each other.

Chamaeodorea pinnatifrons, Wettinia hirsuta, Dictyocaryum fuscum, Aiphanes aculeatta, Bactris simplicifrons and **Geonoma** species produced phytoliths with a fusiform 2D shape, appearing like a club (Fig. S4-sy). Species produced this FUS_ECH morphotype in low amounts of 1–5% (Table S1). There were no significant differences between species for width, sphericity, projections and spinule traits (Supplementary material "Pairwise comparisons").

3.3. Species specific morphotypes

The woody parts sampled of *Geonoma undata* and the seed phytoliths of *A. aculeata* and *Dictyocaryum lamarckianum* produced phytoliths that were not seen in other species (Fig. S4-mr, Table S1). *Geonoma undata* produced phytoliths that were tabular with a variety of 2D shapes (oblong, reniform, ovate, fusiform), an echinate texture and a length and width < 10 μm (Fig. S4-pr). The woody samples of *A. aculeata* (3%) and *Euterpe precatoria* (outside of phytolith count) also contained some small, irregularly shaped phytoliths, but not as much as the woody samples of *Geonoma undata* (>40%). The seed phytoliths of *A. aculeata* had a flattened shape like CON_TAB phytoliths, but lacked an echinate texture, appearing more as an irregular ornated spheroid with a size of ±5 μm (Fig. S4-mn). Such phytoliths comprised 73% of the phytolith count, along with CON_ECH (4%) and CON_TAB (23%). The seed phytoliths of *Dictyocaryum lamarckianum* only contained phytoliths that appeared irregularly ornated spheroids. The seeds of *Euterpe precatoria* and *Dictyocaryum fuscum* and the long seeds of *Dictyocaryum lamarckianium* did not contain such irregular phytoliths. Leaf phytoliths of *Euterpe precatoria* contained the morphotype EUTERPE SPHEROID GRANULATE (EUT_SPH) with a size range between 28 and 38 μm (Fig. S4-aj,ak, Table S1). This morphotype was not found in other species and was counted only once in the phytolith count (Table S1).

4. Discussion

We have assessed the variability of Amazonian palm phytolith morphotypes to determine which traits can be used to increase their

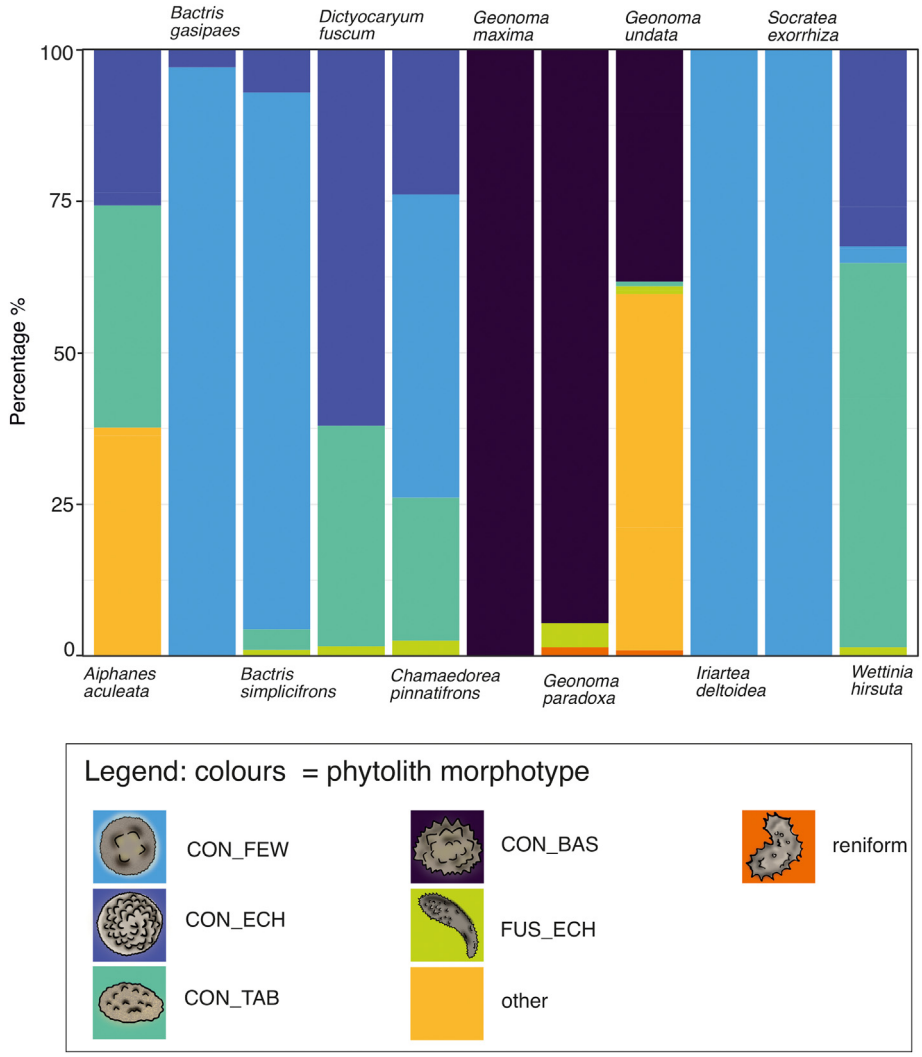

Fig. 4. Relative frequency of conical morphotypes is shown in percentage (%) on the y-axis, with colors showing different morphotypes, and each bar on the x-axis represents a specimen. Based on 300 counted phytoliths per sample.

taxonomic resolution and identification in palaeoecological reconstructions. Several species differed in the size of the phytoliths they produced, and to a lesser extent in shape and spinule traits. But PCA results showed considerable overlap between subfamilies, unlike other studies (Benvenuto et al., 2015). Corresponding with previous research, several genera of palms could be separated based on phytolith morphology or size (Huisman et al., 2018; Morcote-Ríos et al., 2016; Piperno et al., 2019; Piperno and McMichael, 2020).

Spheroid and conical phytoliths differ in size, shape and number of projections and PCA results confirmed the morphotypes that were described for Amazonian and Andean palm phytoliths (Huisman et al., 2018; Morcote-Ríos et al., 2016; Piperno and McMichael, 2020). Species produced these morphotypes in a different frequency: some species, such as *Iriartea deltoidea,* only produced 1 morphotype. Considering different morphotypes, the frequencies in which they are produced, and the different size ranges and means will allow identifying certain taxa: *A. aculeata, Attalea maripa, Bactris simplicifrons, Dictyocaryum fuscum, Euterpe precatoria, Iriartea deltoidea, Oenocarpus bacaba, Socratea exorrhiza* and the genera **Geonoma**, **Bactris**, **Euterpe** and **Oenocarpus**. Therefore, the influence of past human activities and environmental changes through time on palm abundances can be robustly assessed for those taxa. Differences in the modern distribution or edaphic factors may be used to rule in or out species or genera that share phytolith morphotypes (of similar size and shape).

4.1. A guide to identify Amazonian palm phytoliths

4.1.1. Spheroid phytoliths: Size matters

PCA confirmed the morphological differences between the previously established spheroid morphotypes (Morcote-Ríos et al., 2016). Size measurements can be used to increase taxonomic resolution of palm species that produce spheroid phytoliths. Spinule traits were often correlated with size, meaning that larger phytoliths produced spines that were longer, wider and had more distance between spines (Supplementary material "Correlation"). Therefore, focusing on diameter differences between species also implicitly considers spinule traits. We have summarized our findings into a 'Quick Guide' (Fig. 7) to identify palm species producing spheroid phytoliths, for future phytolith research in tropical South America. Future work can refine and modify the guides and include more species.

For SPH_SYM and SPH_TUB morphotypes, separating based on size will allow identifying the larger phytoliths of *Oenocarpus bacaba* and *Attalea maripa.* For SPH_ACU morphotypes, phytoliths > 20 μm are likely produced by **Euterpe** and **Oenocarpus** species (Morcote-Ríos et al., 2016; Piperno et al., 2019; Piperno and McMichael, 2020). *Euterpe oleraceae* also produces SPH_ACU > 20 μm (Piperno and McMichael, 2020). *Mauritiella armata* produced small SPH_ACU phytoliths, and phytoliths that could be small SPH_ACU or SPH_ECH phytoliths with many projections. This might explain why in other studies, *Mauritiella*

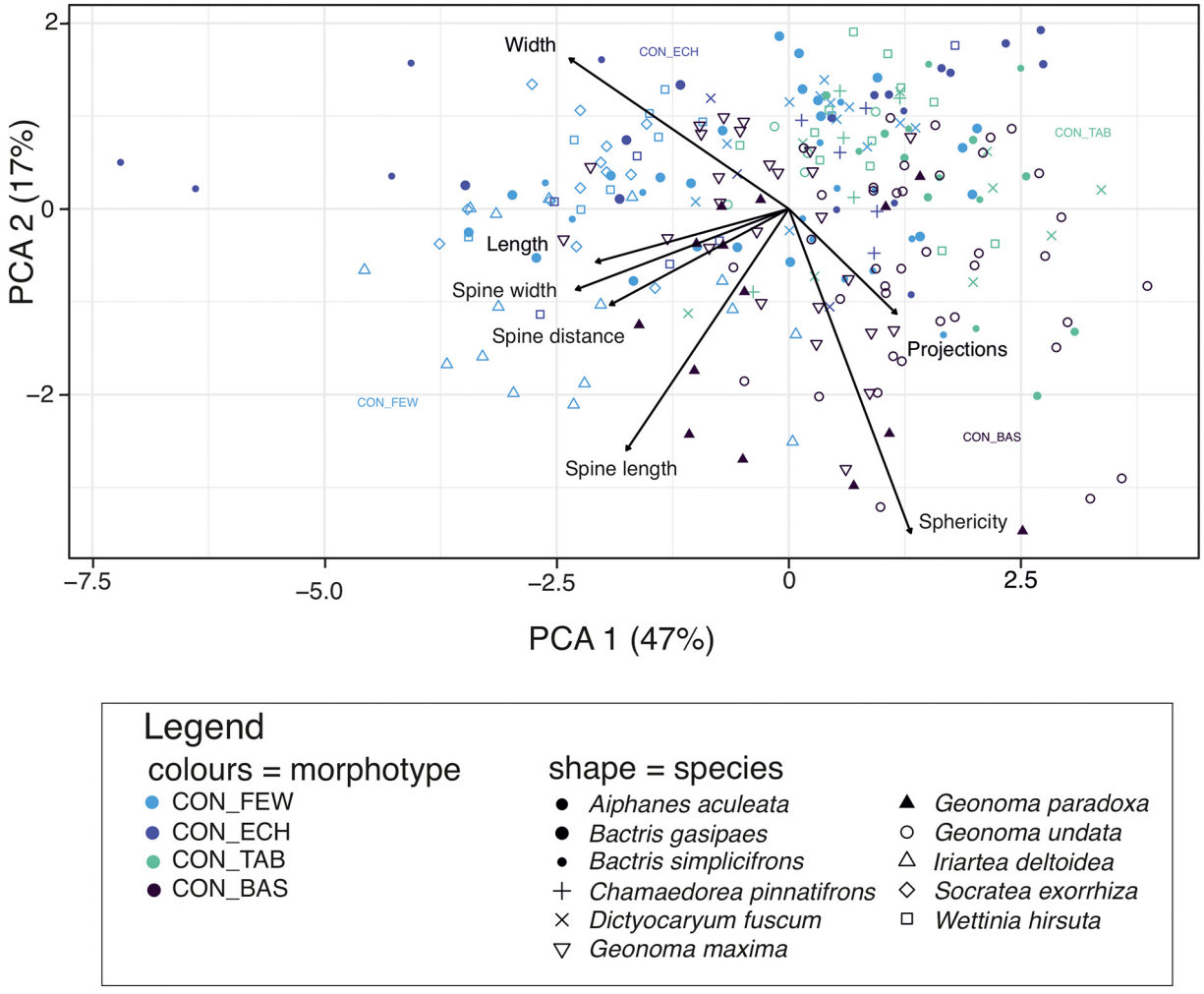

Fig. 5. PCA of conical phytoliths. PCA1 on the x-axis explains 47% of the variance found and PCA2 on the y-axis explains 17%. Different colors indicate conical morphotypes and different shapes indicate species.

armata was not reported to produce SPH_ACU morphotypes (Morcote-Ríos et al., 2016). Small SPH_ACU phytoliths (<15 μm) were also produced by *Attalea speciosa*, and they can also be produced by **Chelyocarpus**, **Manicaria**, **Prestoea** or **Syagrus** species (Morcote-Ríos et al., 2016; Piperno and McMichael, 2020). *Attalea maripa* produced few SPH_ACU phytoliths that resembled large versions of SPH_ECH phytoliths. Because SPH_ECH phytoliths are between 4 and 18 μm long, we categorized these larger phytoliths as SPH_ACU. But other phytolith researchers might categorize them as (large) SPH_ECH.

Lowering taxonomic resolution based on the morphotype of SPH_ECH or ELL_ECH alone is difficult. Differences in the combination of phytoliths produced may help to increase taxonomic resolution for species when globular phytoliths overlap in size. For example, if large SPH_ECH phytoliths are identified in the absence of SPH_SYM phytoliths, it is likely not produced by *Mauritia flexuosa*. Also, *Attalea maripa* is the only species that produces large SPH_ECH, ELL_ECH and SPH_TUB phytoliths (Fig. 7). But given the small number of species studied, such interpretations cannot be made with absolute certainty. Also, using relative frequencies can be difficult in fossil samples when multiple species may have contributed to the phytolith assemblage.

Oenocarpus and **Attalea** species that produced SPH_TUB phytoliths also produced spheroid psilate morphotypes: perhaps these phytoliths represent different stages of spheroid echinate phytolith formation. Similar phytolith morphotypes were found in **Hyphaene** and **Phoenix** species, where authors described the undeveloped morphotypes as part of phytolith genesis (Thomas et al., 2012). But lobate psilate, spheroid psilate and spheroid rugose phytoliths were seen in *Jubaea chilensis, Cocos nucifera* and *Pritchardia perciualarum* without SPH_TUB morphotypes (Delhon and Orliac, 2010), and spheroids with psilate, rugose and ornated textures are also produced by eudicots (Piperno and McMichael, 2020).

Other studies also identified spheroid phytoliths with rounded projections in *Oenocarpus bacaba,* and smaller spheroid phytoliths with rounded projections were seen in *Oenocarpus minor* (Piperno et al., 2021). Future research should study more specimens of **Oenocarpus** to confirm if this morphotype is indicative of the genus. We found no SPH_ACU phytoliths for *Oenocarpus bacaba* and only found SPH_ACU in *Oenocarpus mapora* during extended scans, in contrast to other studies (Piperno and McMichael, 2020), this is likely because this morphotype is produced in rare amounts. A previous study (Morcote-Ríos et al., 2016) reported that *M. flexuosa* produced only SPH_SYM morphotypes, whereas we also identified SPH_ECH phytoliths. *Hyospathe elegans* has been reported to produce only ELL_ECH phytoliths (Morcote-Ríos et al., 2016), whereas in this study, SPH_ECH phytoliths were also identified. These differences highlight the need to study the variation of phytolith traits within multiple individuals of the same species. Another explanation might lay in the eye of the phytolith researcher. To clarify our categories, we have included Figs. S1–S4. Phytolith preservation in fossil samples should also be studied for Amazonian soils and lake sediments, to take a possible preservation bias of phytolith size into account (Albert et al., 2009).

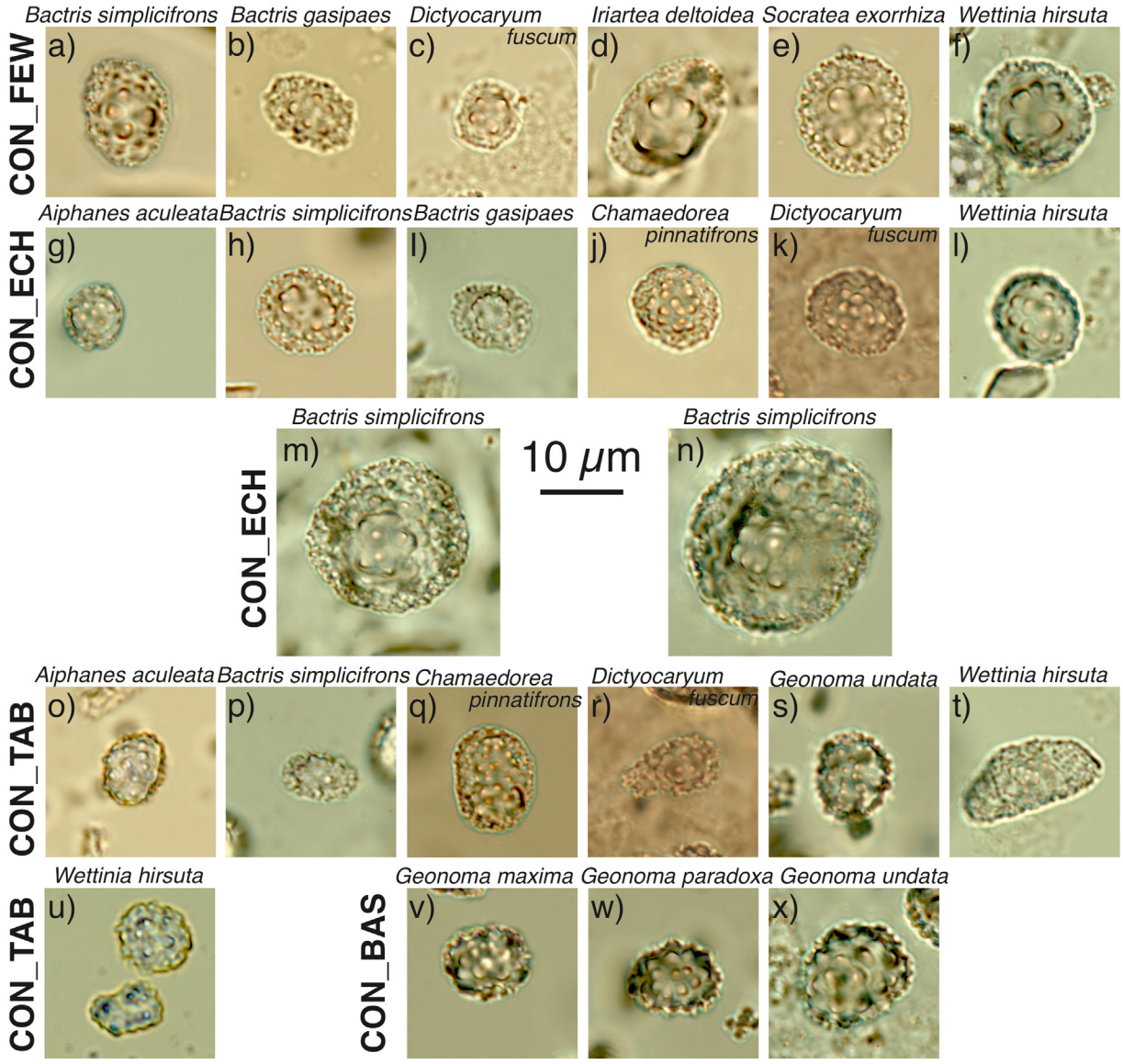

Fig. 6. Variability of conical phytoliths produced by each species: panel a-f shows CON_FEW phytoliths, panels g-n show CON_ECH phytoliths, Panels o-u show CON_TAB phytoliths and panels v-x show CON_BAS phytoliths.

4.1.2. Conical phytoliths: Size and shape matter

PCA confirmed the morphological differences between the 4 conical morphotypes (Huisman et al., 2018). Separating 4 morphotypes will increase taxonomic resolution because species differ in the morphotypes they produce: *Iriartea deltoidea* and *Socratea exorrhiza* produced only CON_FEW, and *Bactris gasipaes* produced only CON_FEW and CON_ECH. CON_BAS morphotypes can be used to identify **Geonoma** species (Huisman et al., 2018; Morcote-Ríos et al., 2016). We have summarized our findings into a 'Quick Guide' (Fig. 8) to identify palm species producing conical phytoliths, for future phytolith research in Amazonia. Future work can refine and modify the guides and include more species.

If CON_FEW phytoliths are separated based on size and shape differences, the larger phytoliths of *Iriartea deltoidea* and *Socratea exorrhiza* and the smaller phytoliths of *Dictyocaryum fuscum* may be identified. Because *Wettinia hirsuta* barely produced CON_FEW phytoliths, this species is excluded from Fig. 8, but it's morphotype is like *Socratea exorrhiza*. We have focused on size and shape differences between CON_FEW morphotypes, because spinule traits reflect size differences and the standard error of the mean overlaps between the number of projections.

If CON_ECH phytoliths are separated based on size differences, the larger phytoliths of *Bactris simplicifrons* and smaller phytoliths of *Aiphanes aculeata* may be identified. Although *Bactris simplicifrons* produces a wide range of CON_ECH phytoliths, it was the only species that produced CON_ECH phytoliths > 17 µm. Also, **Bactris** species produced CON_ECH phytoliths with fewer projections, allowing possible identification of this genus, but more **Bactris** species should be studied to determine this.

Separating CON_TAB phytoliths based on size and shape differences may allow identification of *A. aculeata,* because the mean and median of CON_TAB phytoliths of other species was greater than 10 µm, despite overlap in range. Also, a combination of small CON_ECH and CON_TAB phytoliths likely indicates the presence of *A. aculeata.* Although this was not measured, the top projections of CON_TAB phytoliths produced by *Wettinia hirsuta* seemed less echinate compared to other species (Fig. 6u). Future research should include other **Wettinia** species to study if this texture is characteristic of the genus.

All **Geonoma** species differed in the maximum diameter of CON_BAS phytoliths, but because the ranges overlap and we included only 3 of the 17 **Geonoma** species in Amazonia (Henderson et al., 2019), we have not used this size difference to separate within the **Geonoma** genus.

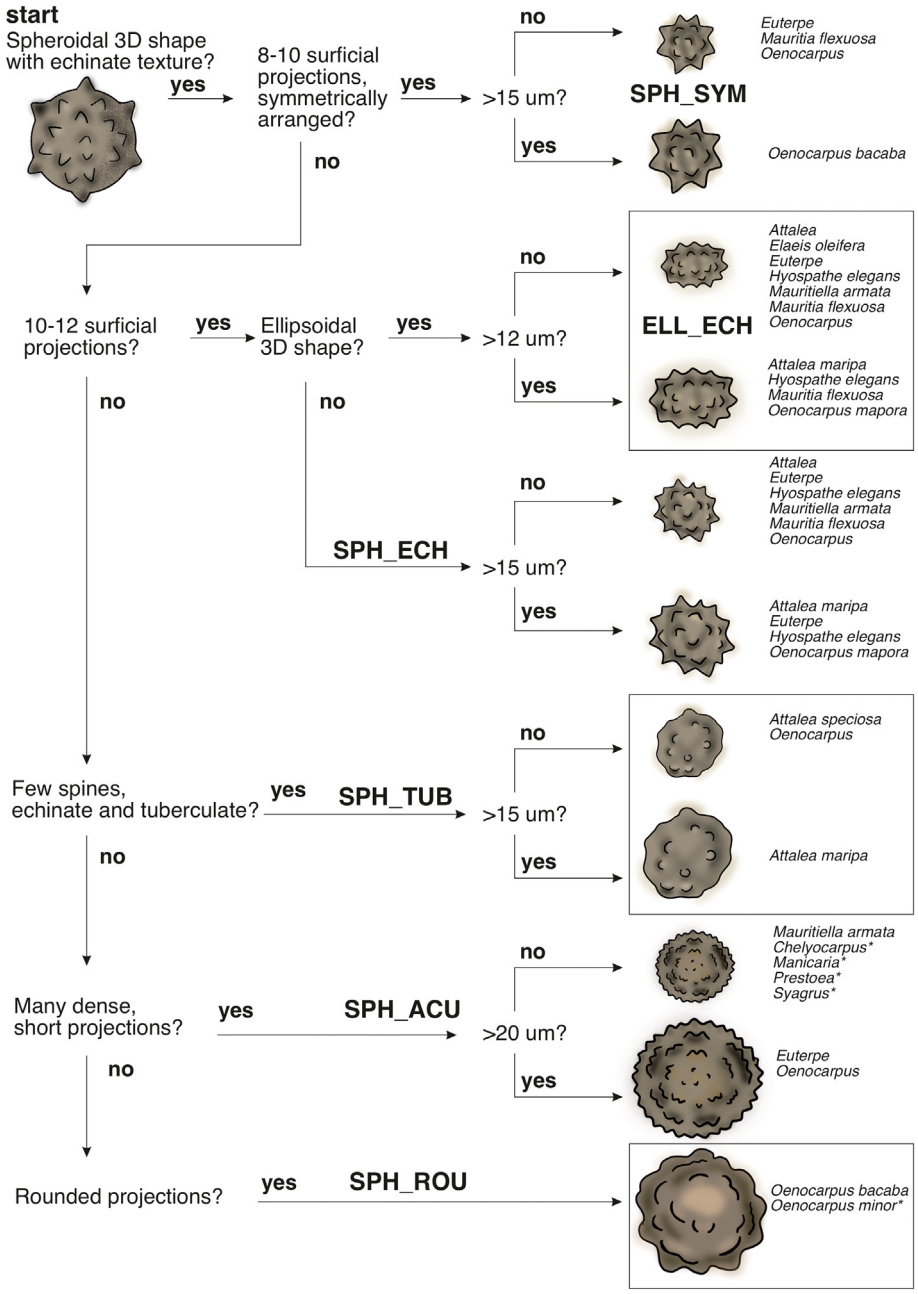

Fig. 7. A quick guide to identify spheroid palm phytoliths under the microscope, using morphological differences in number of surficial projections, size and shape of 12 species and previously established morphotypes (Morcote-Ríos et al., 2016; Piperno and McMichael, 2020).

Phytolith morphotypes produced by previously assessed species were mostly corresponding to the literature (Huisman et al., 2018; Morcote-Ríos et al., 2016; Piperno et al., 2019; Piperno and McMichael, 2020). But there were some differences, such as in the occurrence of reniform phytoliths (Table S1). Phytolith morphotypes produced in rarity might vary more between reference samples and fall outside the phytolith count.

4.2. Other phytolith morphotypes

EUT_SPH phytoliths seem to be indicative of **Euterpe** species (Huisman et al., 2018). Because of the low abundance but large size of EUT_SPH phytoliths, we suggest doing an extended scan at 200X magnification to confirm the presence or absence of this morphotype, outside of the phytolith count. The woody phytoliths of *Geonoma undata* may be species-specific or typical for woody phytoliths, as *A. aculeata* and *Euterpe precatoria* also produced some woody phytoliths (Fig. S4-r). The seed phytoliths of *A. aculeata* and *Dictyocaryum lamarckianum* were not found in other seeds (Fig. S4-mo). The rare FUS_ECH phytoliths produced by several species (Table S1) were similar to woody and seed phytoliths of *Ceroxylon alpinum*, that were reported as malformations (Huisman et al., 2018). This research was not performed with different plant parts per specimen. Sampling more plant parts to create a nested design will reveal if plant parts produce different phytoliths, and if certain morphotypes or malformed phytoliths are typical for seeds or woody parts. Also, the effects of environmental variability on plant growth and subsequent phytolith size must be better studied for positive species-specific identifications to be made based on phytolith size itself.

Another explanation for variation among phytoliths is phylogenetic differences (Faurby et al., 2016). For example, larger CON_FEW

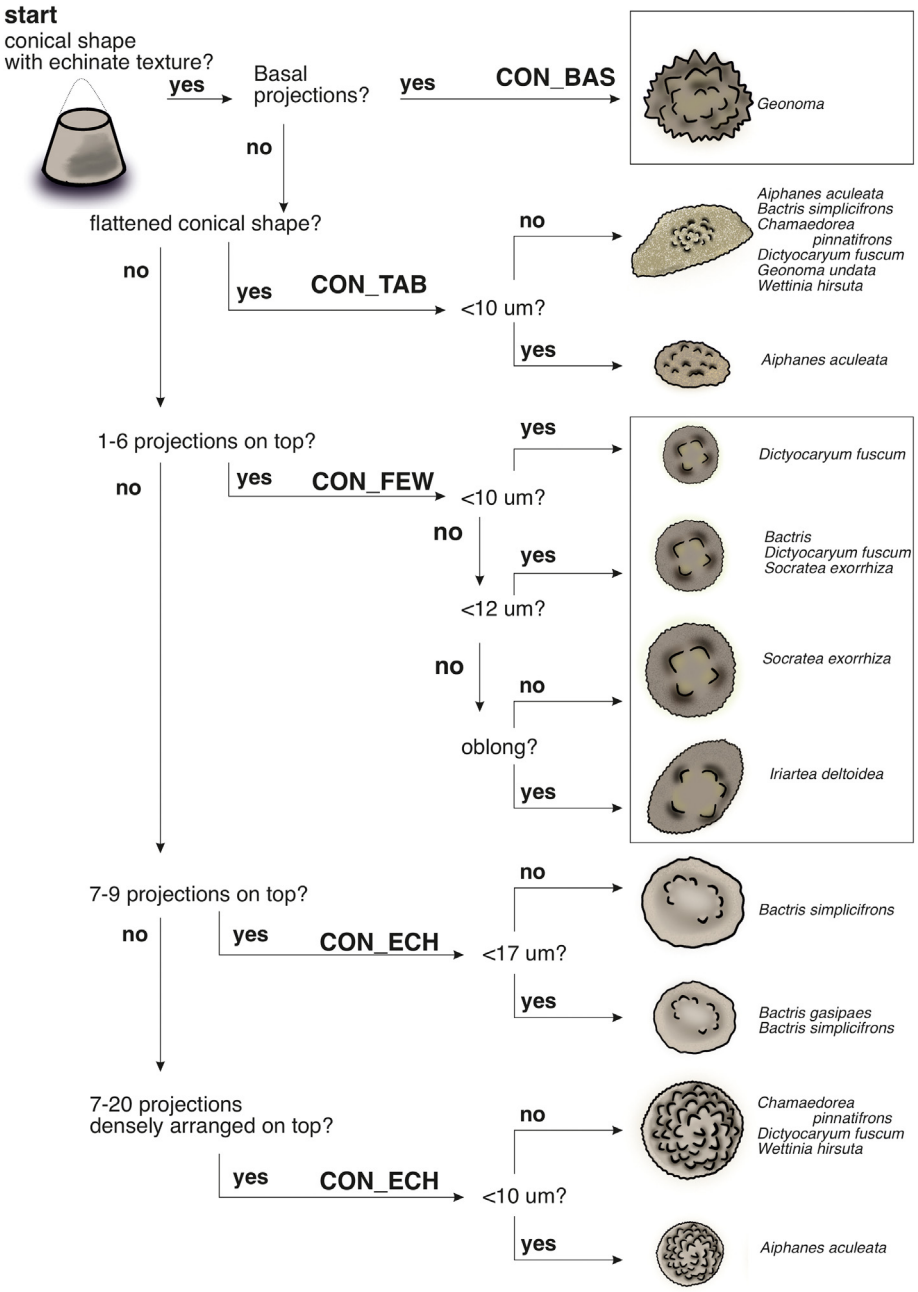

Fig. 8. A quick guide to identify conical palm phytoliths under the microscope, using morphological differences in number of projections, size and shape of 11 species and previously established morphotypes (Huisman et al., 2018; Morcote-Ríos et al., 2016).

morphotypes were restricted to Iriarteae species and CON_BAS phytoliths were restricted to Geonomateae species. Also, CON_ECH phytoliths with 7–9 projections only occurred only in Bactritinidae species and *Aiphanes* produced smaller phytoliths than species from other tribes. Finally, only Euterpeae and Oenocarpus species produced large SPH_ACU phytoliths (>20 μm) (Piperno and McMichael, 2020). But phylogenetic differences alone are unlikely to explain variation in phytolith production, because spheroid phytoliths are produced by several tribes (Euterpeae, Cocoseae and Lepidocaryeae) (Huisman et al., 2018; Morcote-Ríos et al., 2016). Also, variation in size, shape or number of projections varied widely within a genus. Studying the phytoliths of **Astryocaryum** and **Desmoncus** species, who are closely related to **Bactris** and **Aiphanes**, might shine light on the role of phylogenetic relatedness in the morphology of conical phytoliths.

4.3. Future palaeoecological research

The quick guides of spheroid and conical phytoliths (Figs. 7, 8) can be used to in future phytolith analyses to reconstruct the distribution and abundance of specific palm species and genera through time, improving our ability to understand how people and the environmental context have shaped the widespread occurrence of Amazonian palm species. Our results allow separating the past histories of palm species used for their trunks (such as *Iriartea deltoidea, Socratea exorrhiza)* from palm species used for food (such as *Euterpe precatoria)*, which is useful, because people may have locally depleted species used for wood but increased the abundance of palm species they ate. Understanding the role of past human activities, such as agroforestry, on modern palm abundance and occurrence, will help to understand the

temporal and spatial scale of past human impact in Amazonia, which is a highly debated (Levis et al., 2017; Lombardo et al., 2020; McMichael et al., 2017; Piperno et al., 2021, 2019).

Given the large number of palm species used in Amazonia (currently 134), expanding this dataset of phytolith traits from reference material with species such as *Astryocaryum murumuru* or *Phytelephas macrocarpa* will be of great value to those studying Amazonian phytoliths (and the role of past human activities). Because this dataset only contains 30 phytoliths per sample, expanding this dataset is necessary to allow more robust statistical analysis. Because measuring and counting phytolith is labour intensive, the automatic classification of phytolith morphometrics may be a promising area for future research.

5. Conclusion

Although only 24 Amazonian palm species were included in this research, results show potential for phytoliths of the following species to be identified on the basis of their size, shape or number of projections: *A. aculeata, Attalea maripa, Bactris simplicifrons, Dictyocaryum fuscum, Euterpe precatoria, Iriartea deltoidea, Oenocarpus bacaba, Socratea exorrhiza* and the genera **Geonoma, Bactris, Euterpe** and **Oenocarpus**. This will allow future phytolith analyses to reconstruct past vegetations with an increased taxonomic resolution, especially of hyperdominant and useful palms. We recommend that more specimens of some of these species should be studied to determine if phytolith morphology is sensitive to environmental variability. However, it appears that important economic species of **Oenocarpus** and **Euterpe**, O. *bataua* and *Emesaya precatoria*, consistently produce SPH_ACU phytoliths larger in size (>20 μm) than in some congenerics and other SPH_ACU-producing taxa studied so far, as plants sampled from different areas of Amazonia showed little phytolith size difference when compared with our results (Morcote-Ríos et al., 2016; Piperno and McMichael, 2020). The growing number of vegetation inventories being carried out in lowland Amazonia and knowledge of where different species are distributed due to edaphic or other preferences may also allow greater taxonomic resolution (Piperno et al., 2021). The quick guides of Figs. 7 and 8 can be used to test hypotheses regarding the abundance and occurrence of Amazonian palms and the possible influence of past human activities.

Supplementary data to this article can be found online at https://doi.org/10.1016/j.revpalbo.2022.104613.

Declaration of Competing Interest

The authors declare that they have no known competing financial interests or personal relationships that could have appeared to influence the work reported in this paper.

Acknowledgements

C.N.H.M. and N.H.W. would like to thank European Research Council Starting Grant StG 853394 (2019) for funding for this work. We would like to thank Huasheng Huang for his suggestions regarding the phytolith photographs. We would like to thank Marnel Scherrenberg from the Herbarium in Leiden and Reinout Havinga from the Hortus Botanicus Amsterdam for providing us with plant material.

References

Abràmoff, M.D., Magalhães, P.J., Ram, S.J., 2004. Image processing with imageJ. Biophotonics Int. 11, 36–41. https://doi.org/10.1201/9781420005615.ax4.

Åkesson, C.M., McMichael, C.N.H., Raczka, M.F., Huisman, S.N., Palmeira, M., Vogel, J., Neill, D., Veizaj, J., Bush, M.B., 2021. Long-term ecological legacies in western Amazonia. J. Ecol. 109, 432–446. https://doi.org/10.1111/1365-2745.13501.

Albert, R.M., Bamford, M.K., Cabanes, D., 2009. Palaeoecological significance of palms at Olduvai Gorge, Tanzania, based on phytolith remains. Quat. Int. 193, 41–48.

Ball, T.B., Davis, A., Evett, R.R., Ladwig, J.L., Tromp, M., Out, W.A., Portillo, M., 2016. Morphometric analysis of phytoliths: recommendations towards standardization from the International Committee for Phytolith Morphometrics. J. Archaeol. Sci. 68, 106–111.

Benvenuto, M.L., Fernández Honaine, M., Osterrieth, M.L., Morel, E., 2015. Differentiation of globular phytoliths in Arecaceae and other monocotyledons: Morphological description for paleobotanical application. Turk. J. Bot. 39, 341–353. https://doi.org/10.3906/bot-1312-72.

Chen, S.T., Smith, S.Y., 2013. Phytolith variability in Zingiberales: a tool for the reconstruction of past tropical vegetation. Palaeogeogr. Palaeoclimatol. Palaeoecol. 370, 1–12. https://doi.org/10.1016/j.palaeo.2012.10.026.

Clement, C.R., 1988. Domestication of the Pejibaye Palm (*Bactris gasipaes*). Past and Present 6, 155–174.

Collura, L.V., Neumann, K., 2017. Wood and bark phytoliths of West African woody plants. Quat. Int. 434, 142–159. https://doi.org/10.1016/j.quaint.2015.12.070.

Delhon, C., Orliac, C., 2010. The vanished palm trees of Easter Island: New radiocarbon and phytolith data. Pap. from VII Int. Conf. Easter Isl. Pacific Migr. Identity, Cult. Herit, pp. 97–110.

Eiserhardt, W.L., Svenning, J.C., Kissling, W.D., Balslev, H., 2011. Geographical ecology of the palms (Arecaceae): determinants of diversity and distributions across spatial scales. Ann. Bot. 108, 1391–1416. https://doi.org/10.1093/aob/mcr146.

Faurby, S., Eiserhardt, W.L., Baker, W.J., Svenning, J.C., 2016. An all-evidence species-level supertree for the palms (Arecaceae). Mol. Phylogenet. Evol. 100, 57–69. https://doi.org/10.1016/j.ympev.2016.03.002.

Fauset, S., Johnson, M.O., Gloor, M., Baker, T.R., Monteagudo, M.A., Brienen, R.J.W., Feldpausch, T.R., Lopez-Gonzalez, G., Malhi, Y., Ter Steege, H., Pitman, N.C.A., Baraloto, C., Engel, J., Pétronelli, P., Andrade, A., Camargo, J.L.C., Laurance, S.G.W., Laurance, W.F., Chave, J., Allie, E., Vargas, P.N., Terborgh, J.W., Ruokolainen, K., Silveira, M., Aymard, C., G.A, Arroyo, L., Bonal, D., Ramirez-Angulo, H., Araujo-Murakami, A., Neill, D., Hérault, B., Dourdain, A., Torres-Lezama, A., Marimon, B.S., Salomão, R.P., Comiskey, J.A., Réjou-Méchain, M., Toledo, M., Licona, J.C., Alarcón, A., Prieto, A., Rudas, A., Van Der Meer, P.J., Killeen, T.J., Marimon Junior, B.H., Poorter, L., Boot, R.G.A., Stergios, B., Torre, E.V., Costa, F.R.C., Levis, C., Schietti, J., Souza, P., Groot, N., Arets, E., Moscoso, V.C., Castro, W., Coronado, E.N.H., Peña-Claros, M., Stahl, C., Barroso, J., Talbot, J., Vieira, I.C.G., Van Der Heijden, G., Thomas, R., Vos, V.A., Almeida, E.C., Davila, E.Á., Aragão, L.E.O.C., Erwin, T.L., Morandi, P.S., De Oliveira, E.A., Valadão, M.B.X., Zagt, R.J., Van Der Hout, P., Loayza, P.A., Pipoly, J.J., Wang, O., Alexiades, M., Cerón, C.E., Huamantupa-Chuquimaco, I., Di Fiore, A., Peacock, J., Camacho, N.C.P., Umetsu, R.K., De Camargo, P.B., Burnham, R.J., Herrera, R., Quesada, C.A., Stropp, J., Vieira, S.A., Steininger, M., Rodríguez, C.R., Restrepo, Z., Muelbert, A.E., Lewis, S.L., Pickavance, G.C., Phillips, O.L., 2015. Hyperdominance in Amazonian forest carbon cycling. Nat. Commun. 6, 1–9. https://doi.org/10.1038/ncomms7857.

Fenwick, R.S.H., Lentfer, C.J., Weisler, M.I., 2011. Palm reading: a pilot study to discriminate phytoliths of four Arecaceae (Palmae) taxa. J. Archaeol. Sci. 38, 2190–2199. https://doi.org/10.1016/j.jas.2011.03.016.

Garnier, S., Ross, N., Rudis, R., Camargo, P.A., Sciaini, M., Scherer, C., 2021. {viridis} - Colorblind-Friendly Color Maps for R. https://doi.org/10.5281/zenodo.4679424.

Goulding, M., Smith, N., others, 2007. Palms: Sentinels for Amazon Conservation. Missouri Botanical Garden Press.

Heijink, B.M., McMichael, C.N.H., Piperno, D.R., Duivenvoorden, J.F., Cárdenas, D., Duque, Á., 2020. Holocene increases in palm abundances in north-western Amazonia. J. Biogeogr. 47, 698–711.

Henderson, A., Galeano, G., Bernal, R., 2019. Field Guide to the Palms of the Americas. Princeton University Press.

Huisman, S.N., Raczka, M.F., McMichael, C.N.H., 2018. Palm phytoliths of mid-elevation Andean forests. Front. Ecol. Evol. 6, 1–8. https://doi.org/10.3389/fevo.2018.00193.

Kassambara, A., Mundt, F., 2017. Package 'factoextra.'. Extr. Vis. results Multivar. data Anal, p. 76.

Kristiansen, T., Svenning, J.C., Grández, C., Salo, J., Balslev, H., 2009. Commonness of Amazonian palm (Arecaceae) species: Cross-scale links and potential determinants. Acta Oecol. 35, 554–562. https://doi.org/10.1016/j.actao.2009.05.001.

Levis, C., Costa, F.R.C., Bongers, F., Peña-Claros, M., Clement, C.R., Junqueira, A.B., Neves, E.G., Tamanaha, E.K., Figueiredo, F.O.G., Salomão, R.P., others, 2017. Persistent effects of pre-Columbian plant domestication on Amazonian forest composition. Science (80-.) 355, 925–931.

Lombardo, U., Iriarte, J., Hilbert, L., Ruiz-Pérez, J., Capriles, J.M., Veit, H., 2020. Early Holocene crop cultivation and landscape modification in Amazonia. Nature 581, 190–193. https://doi.org/10.1038/s41586-020-2162-7.

Macia, M.J., Armesilla, P.J., Cámara-Leret, R., Paniagua-Zambrana, N., Villalba, S., Balslev, H., Pardo-de-Santayana, M., 2011. Palm uses in northwestern South America: a quantitative review. Bot. Rev. 77, 462–570.

Maezumi, S.Y., Alves, D., Robinson, M., de Souza, J.G., Levis, C., Barnett, R.L., Almeida de Oliveira, E., Urrego, D., Schaan, D., Iriarte, J., 2018. The legacy of 4,500 years of polyculture agroforestry in the eastern Amazon. Nat. Plants 4, 540–547. https://doi.org/10.1038/s41477-018-0205-y.

McMichael, C.H., Piperno, D.R., Bush, M.B., Silman, M.R., Zimmerman, A.R., Raczka, M.F., Lobato, L.C., 2012. Sparse pre-Columbian human habitation in Western Amazonia. Science (80-.)). 336, 1429–1431. https://doi.org/10.1126/science.1219982.

McMichael, C.H., Piperno, D.R., Neves, E.G., Bush, M.B., Almeida, F.O., Mongeló, G., Eyjolfsdottir, M.B., 2015. Phytolith assemblages along a gradient of ancient human disturbance in Western Amazonia. Front. Ecol. Evol. 3, 1–15. https://doi.org/10.3389/fevo.2015.00141.

McMichael, C.H., Feeley, K.J., Dick, C.W., Piperno, D.R., Bush, M.B., 2017. Comment on "persistent effects of pre-Columbian plant domestication on Amazonian forest composition.". Science (80-.) 358, 1–3. https://doi.org/10.1126/science.aan8347.

McMichael, C.N.H., Witteveen, N.H., Scholz, S., Zwier, M., Prins, M.A., Lougheed, B.C., Mothes, P., Gosling, W.D., 2021. 30,000 years of landscape and vegetation dynamics

in a mid-elevation Andean valley. Quat. Sci. Rev. 258, 106866. https://doi.org/10.1016/j.quascirev.2021.106866.
Morcote-Rios, G., Bernal, R., 2001. Remains of palms (Palmae) at archaeological sites in the New World: a review. Bot. Rev. 67, 309–350.
Morcote-Ríos, G., Bernal, R., Raz, L., 2016. Phytoliths as a tool for archaeobotanical, palaeobotanical and palaeoecological studies in Amazonian palms. Bot. J. Linn. Soc. 182, 348–360. https://doi.org/10.1111/boj.12438.
Muscarella, R., Emilio, T., Phillips, O.L., Lewis, S.L., Slik, F., Baker, W.J., Couvreur, T.L.P., Eiserhardt, W.L., Svenning, J.C., Affum-Baffoe, K., Aiba, S.I., de Almeida, E.C., de Almeida, S.S., de Oliveira, E.A., Álvarez-Dávila, E., Alves, L.F., Alvez-Valles, C.M., Carvalho, F.A., Guarin, F.A., Andrade, A., Aragão, L.E.O.C., Murakami, A.A., Arroyo, L., Ashton, P.S., Corredor, G.A.A., Baker, T.R., de Camargo, P.B., Barlow, J., Bastin, J.F., Bengone, N.N., Berenguer, E., Berry, N., Blanc, L., Böhning-Gaese, K., Bonal, D., Bongers, F., Bradford, M., Brambach, F., Brearley, F.Q., Brewer, S.W., Camargo, J.L.C., Campbell, D.G., Castilho, C.V., Castro, W., Catchpole, D., Cerón Martínez, C.E., Chen, S., Chhang, P., Cho, P., Chutipong, W., Clark, C., Collins, M., Comiskey, J.A., Medina, M.N.C., Costa, F.R.C., Culmsee, H., David-Higuita, H., Davidar, P., del Aguila-Pasquel, J., Derroire, G., Di Fiore, A., Van Do, T., Doucet, J.L., Dourdain, A., Drake, D.R., Ensslin, A., Erwin, T., Ewango, C.E.N., Ewers, R.M., Fauset, S., Feldpausch, T.R., Ferreira, J., Ferreira, L.V., Fischer, M., Franklin, J., Fredriksson, G.M., Gillespie, T.W., Gilpin, M., Gonmadje, C., Gunatilleke, A.U.N., Hakeem, K.R., Hall, J.S., Hamer, K.C., Harris, D.J., Harrison, R.D., Hector, A., Hemp, A., Herault, B., Pizango, C.G.H., Coronado, E.N.H., Hubau, W., Hussain, M.S., Ibrahim, F.H., Imai, N., Joly, C.A., Joseph, S., Anitha, K., Kartawinata, K., Kassi, J., Killeen, T.J., Kitayama, K., Klitgård, B.B., Kooyman, R., Labrière, N., Larney, E., Laumonier, Y., Laurance, S.G., Laurance, W.F., Lawes, M.J., Levesley, A., Lisingo, J., Lovejoy, T., Lovett, J.C., Lu, X., Lykke, A.M., Magnusson, W.E., Mahayani, N.P.D., Malhi, Y., Mansor, A., Peña, J.L.M., Marimon-Junior, B.H., Marshall, A.R., Melgaco, K., Bautista, C.M., Mihindou, V., Millet, J., Milliken, W., Mohandass, D., Mendoza, A.L.M., Mugerwa, B., Nagamasu, H., Nagy, L., Seuaturien, N., Nascimento, M.T., Neill, D.A., Neto, L.M., Nilus, R., Vargas, M.P.N., Nurtjahya, E., de Araújo, R.N.O., Onrizal, O., Palacios, W.A., Palacios-Ramos, S., Parren, M., Paudel, E., Morandi, P.S., Pennington, R.T., Pickavance, G., Pipoly, J.J., Pitman, N.C.A., Poedjirahajoe, E., Poorter, L., Poulsen, J.R., Rama Chandra Prasad, P., Prieto, A., Puyravaud, J.P., Qie, L., Quesada, C.A., Ramírez-Angulo, H., Razafimahaimodison, J.C., Reitsma, J.M., Requena-Rojas, E.J., Correa, Z.R., Rodriguez, C.R., Roopsind, A., Rovero, F., Rozak, A., Lleras, A.R., Rutishauser, E., Rutten, G., Punchi-Manage, R., Salomão, R.P., Van Sam, H., Sarker, S.K., Satdichanh, M., Schietti, J., Schmitt, C.B., Marimon, B.S., Senbeta, F., Nath Sharma, L., Sheil, D., Sierra, R., Silva-Espejo, J.E., Silveira, M., Sonké, B., Steininger, M.K., Steinmetz, R., Stévart, T., Sukumar, R., Sultana, A., Sunderland, T.C.H., Suresh, H.S., Tang, J., Tanner, E., ter Steege, H., Terborgh, J.W., Theilade, I., Timberlake, J., Torres-Lezama, A., Umunay, P., Uriarte, M., Gamarra, L.V., van de Bult, M., van der Hout, P., Martinez, R.V., Vieira, I.C.G., Vieira, S.A., Vilanova, E., Cayo, J.V., Wang, O., Webb, C.O., Webb, E.L., White, L., Whitfeld, T.J.S., Wich, S., Willcock, S., Wiser, S.K., Young, K.R., Zakaria, R., Zang, R., Zartman, C.E., Zo-Bi, I.C., Balslev, H., 2020. The global abundance of tree palms. Glob. Ecol. Biogeogr. 1–20.
Neumann, K., Strömberg, C.A.E., Ball, T., Albert, R.M., Vrydaghs, L., Cummings, L.S., 2019. International Code for Phytolith Nomenclature (ICPN) 2.0. Ann. Bot. 124, 189–199. https://doi.org/10.1093/aob/mcz064.
Piperno, D.R., 1989. Phytolith Analysis: An Archaeological and Geological Perspective. Elsevier, Man https://doi.org/10.2307/2802711.
Piperno, D.R., 2006. Phytoliths: A Comprehensive Guide for Archaeologists and Paleoecologists. Rowman Altamira.
Piperno, D.R., McMichael, C., 2020. Phytoliths in modern plants from Amazonia and the neotropics at large: implications for vegetation history reconstruction. Quat. Int. 565, 54–74. https://doi.org/10.1016/j.quaint.2020.10.043.
Piperno, D.R., McMichael, C.N.H., Bush, M.B., 2019. Finding forest management in prehistoric Amazonia. Anthropo. 26, 100211.
Piperno, D.R., Mcmichael, C.H., Pitman, N.C.A., Guevara Andino, J.E., Paredes, M.R., Heijink, C.B.M., Torres-Montenegro, L.A., Performed, B.M.H., Analyzed Data, T.-M, 2021. A 5,000-year vegetation and fire history for tierra firme forests in the Medio Putumayo-Algodón watersheds, northeastern Peru. Proc. Natl. Acad. Sci. 118. https://doi.org/10.1073/pnas.2022213118/-/DCSupplemental.Published 2022213118.
Ter Steege, H., Pitman, N.C.A., Sabatier, D., Baraloto, C., Salomão, R.P., Guevara, J.E., Phillips, O.L., Castilho, C.V., Magnusson, W.E., Molino, J.F., Monteagudo, A., Vargas, P.N., Montero, J.C., Feldpausch, T.R., Coronado, E.N.H., Killeen, T.J., Mostacedo, B., Vasquez, R., Assis, R.L., Terborgh, J., Wittmann, F., Andrade, A., Laurance, W.F., Laurance, S.G.W., Marimon, B.S., Marimon, B.H., Vieira, I.C.G., Amaral, I.L., Brienen, R., Castellanos, H., López, D.C., Duivenvoorden, J.F., Mogollón, H.F., Matos, F.D.D.A., Dávila, N., García-Villacorta, R., Diaz, P.R.S., Costa, F., Emilio, T., Levis, C., Schietti, J., Souza, P., Alonso, A., Dallmeier, F., Montoya, A.J.D., Piedade, M.T.F., Araujo-Murakami, A., Arroyo, L., Gribel, R., Fine, P.V.A., Peres, C.A., Toledo, M., Aymard, C.G.A., Baker, T.R., Cerón, C., Engel, J., Henkel, T.W., Maas, P., Petronelli, P., Stropp, J., Zartman, C.E., Daly, D., Neill, D., Silveira, M., Paredes, M.R., Chave, J., Lima Filho, D.D.A., Jørgensen, P.M., Fuentes, A., Schöngart, J., Valverde, F.C., Di Fiore, A., Jimenez, E.M., Mora, M.C.P., Phillips, J.F., Rivas, G., Van Andel, T.R., Von Hildebrand, P., Hoffman, B., Zent, E.L., Malhi, Y., Prieto, A., Rudas, A., Ruschell, A.R., Silva, N., Vos, V., Zent, S., Oliveira, A.A., Schutz, A.C., Gonzales, T., Nascimento, M.T., Ramirez-Angulo, H., Sierra, R., Tirado, M., Medina, M.N.U., Van Der Heijden, G., Vela, C.I.A., Torre, E.V., Vriesendorp, C., Wang, O., Young, K.R., Baider, C., Balslev, H., Ferreira, C., Mesones, I., Torres-Lezama, A., Giraldo, L.E.U., Zagt, R., Alexiades, M.N., Hernandez, L., Huamantupa-Chuquimaco, I., Milliken, W., Cuenca, W.P., Pauletto, D., Sandoval, E.V., Gamarra, L.V., Dexter, K.G., Feeley, K., Lopez-Gonzalez, G., Silman, M.R., 2013. Hyperdominance in the Amazonian tree flora. Science (80-.), 342 https://doi.org/10.1126/science.1243092.
ter Steege, H., Prado, P.I., Lima, R.A.F.d., Pos, E., de Souza Coelho, L., de Andrade Lima Filho, D., Salomão, R.P., Amaral, I.L., de Almeida Matos, F.D., Castilho, C.V., Phillips, O.L., Guevara, J.E., de Jesus Veiga Carim, M., Cárdenas López, D., Magnusson, W.E., Wittmann, F., Martins, M.P., Sabatier, D., Irume, M.V., da Silva Guimarães, J.R., Molino, J.F., Bánki, O.S., Piedade, M.T.F., Pitman, N.C.A., Ramos, J.F., Monteagudo Mendoza, A., Venticinque, E.M., Luize, B.G., Núñez Vargas, P., Silva, T.S.F., de Leão Novo, E.M.M., Reis, N.F.C., Terborgh, J., Manzatto, A.G., Casula, K.R., Honorio Coronado, E.N., Montero, J.C., Duque, A., Costa, F.R.C., Castaño Arboleda, N., Schöngart, J., Zartman, C.E., Killeen, T.J., Marimon, B.S., Marimon-Junior, B.H., Vasquez, R., Mostacedo, B., Demarchi, L.O., Feldpausch, T.R., Engel, J., Petronelli, P., Baraloto, C., Assis, R.L., Castellanos, H., Simon, M.F., de Medeiros, M.B., Quaresma, A., Laurance, S.G.W., Rincón, L.M., Andrade, A., Sousa, T.R., Camargo, J.L., Schietti, J., Laurance, W.F., de Queiroz, H.L., Nascimento, H.E.M., Lopes, M.A., de Sousa Farias, E., Magalhães, J.L.L., Brienen, R., Aymard, C.G.A., Revilla, J.D.C., Vieira, I.C.G., Cintra, B.B.L., Stevenson, P.R., Feitosa, Y.O., Duivenvoorden, J.F., Mogollón, H.F., Araujo-Murakami, A., Ferreira, L.V., Lozada, J.R., Comiskey, J.A., de Toledo, J.J., Damasco, G., Dávila, N., Lopes, A., García-Villacorta, R., Draper, F., Vicentini, A., Cornejo Valverde, F., Lloyd, J., Gomes, V.H.F., Neill, D., Alonso, A., Dallmeier, F., de Souza, F.C., Gribel, R., Arroyo, L., Carvalho, F.A., de Aguiar, D.P.P., do Amaral, D.D., Pansonato, M.P., Feeley, K.J., Berenguer, E., Fine, P.V.A., Guedes, M.C., Barlow, J., Ferreira, J., Villa, B., Peñuela Mora, M.C., Jimenez, E.M., Licona, J.C., Cerón, C., Thomas, R., Maas, P., Silveira, M., Henkel, T.W., Stropp, J., Paredes, M.R., Dexter, K.G., Daly, D., Baker, T.R., Huamantupa-Chuquimaco, I., Milliken, W., Pennington, T., Tello, J.S., Pena, J.L.M., Peres, C.A., Klitgaard, B., Fuentes, A., Silman, M.R., Di Fiore, A., von Hildebrand, P., Chave, J., van Andel, T.R., Hilário, R.R., Phillips, J.F., Rivas-Torres, G., Noronha, J.C., Prieto, A., Gonzales, T., de Sá Carpanedo, R., Gonzales, G.P.G., Gómez, R.Z., de Jesus Rodrigues, D., Zent, E.L., Ruschel, A.R., Vos, V.A., Fonty, É., Junqueira, A.B., Doza, H.P.D., Hoffman, B., Zent, S., Barbosa, E.M., Malhi, Y., de Matos Bonates, L.C., de Andrade Miranda, I.P., Silva, N., Barbosa, F.R., Vela, C.I.A., Pinto, L.F.M., Rudas, A., Albuquerque, B.W., Umaña, M.N., Carrero Márquez, Y.A., van der Heijden, G., Young, K.R., Tirado, M., Correa, D.F., Sierra, R., Costa, J.B.P., Rocha, M., Vilanova Torre, E., Wang, O., Oliveira, A.A., Kalamandeen, M., Vriesendorp, C., Ramirez-Angulo, H., Holmgren, M., Nascimento, M.T., Galbraith, D., Flores, B.M., Scudeller, V.V., Cano, A., Ahuite Reategui, M.A., Mesones, I., Baider, C., Mendoza, C., Zagt, R., Urrego Giraldo, L.E., Ferreira, C., Villarroel, D., Linares-Palomino, R., Farfan-Rios, W., Farfan-Rios, W., Casas, L.F., Cárdenas, S., Balslev, H., Torres-Lezama, A., Alexiades, M.N., Garcia-Cabrera, K., Valenzuela Gamarra, L., Valderrama Sandoval, E.H., Ramirez Arevalo, F., Hernandez, L., Sampaio, A.F., Pansini, S., Palacios Cuenca, W., de Oliveira, E.A., Pauletto, D., Levesley, A., Melgaço, K., Pickavance, G., 2020. Biased-corrected richness estimates for the Amazonian tree flora. Sci. Rep. 10, 1–13. https://doi.org/10.1038/s41598-020-66686-3.
Thomas, R., Tengberg, M., Moulhérat, C., Marcon, V., Besenval, R., 2012. Analysis of a protohistoric net from Shahi Tump, Baluchistan (Pakistan). Archaeol. Anthropol. Sci. 4, 15–23. https://doi.org/10.1007/s12520-011-0078-8.
Tomlinson, P.B., 1961. Anatomy of the monocotyledons. II. Palmae Anatomy of the monocotyledons. II. Palmae.
Vormisto, J., Svenning, J.-C., Hall, P., Balslev, H., 2004. Diversity and dominance in palm (Arecaceae) communities in terra firme forests in the western Amazon basin. J. Ecol. 92, 577–588.
Watling, J., Iriarte, J., 2013. Phytoliths from the coastal savannas of French Guiana. Quat. Int. 287, 162–180. https://doi.org/10.1016/j.quaint.2012.10.030.
Whitney, B.S., Dickau, R., Mayle, F.E., Walker, J.H., Soto, J.D., Iriarte, J., 2014. Pre-Columbian raised-field agriculture and land use in the Bolivian Amazon. Holocene 24, 231–241. https://doi.org/10.1177/0959683613517401.